Supporting Information

Five Water-Soluble Zwitterionic Copper(II)-Carboxylate Polymers: Role of Dipyridyl Coligands in Enhancing the DNA-Binding, Cleaving and Anticancer Activities

Ming Chen, Xiao-Yan Tang, Shui-Ping Yang, Huan-HuanLi, Hai-Qing Zhao, Zhi-Hong Jiang, Jin-Xiang Chen,* Wen-Hua Chen*

Figure Legends:

Table S1. Selected bond distances (Å) and angles (°) for complexes **1-5**.

Fig. S1. The double layered structure linked by secondary bond of Cu···O in $\{[Cu_3(Cmdcp)_2(HO)_2(H_2O)_2]\cdot H_2O\}_n$ (**1**).

Fig. S2. The infinite two-dimensional structure in **3** looking along the *c* axis and all the hydrogen atoms and bipy molecules are omitted for clarity.

Fig. S3. The effect of the addition of complex **1** on the emission intensity of the CT DNA-bound ethidium bromide (3.03 μM) at different complex concentrations in a 5 mM Tri-HCl-50 mM NaCl buffer at pH 7.0 and at room temperature.

Fig. S4. The effect of the addition of complex **2** on the emission intensity of the CT DNA-bound ethidium bromide (3.03 μM) at different complex concentrations in a 5 mM Tri-HCl-50 mM NaCl buffer at pH 7.0 and at room temperature.

Fig. S5. The effect of the addition of complex **3** on the emission intensity of the CT DNA-bound ethidium bromide (3.03 μM) at different complex concentrations in a 5 mM Tri-HCl-50 mM NaCl buffer at pH 7.0 and at room temperature.

Fig. S6. The effect of the addition of complex **4** on the emission intensity of the CT DNA-bound ethidium bromide (3.03 μM) at different complex concentrations in a 5 mM Tri-HCl-50 mM NaCl buffer at pH 7.0 and at room temperature.

Fig. S7. The effect of the addition of complex **5** on the emission intensity of the CT DNA-bound

ethidium bromide (3.03 μM) at different complex concentrations in a 5 mM Tri-HCl-50 mM NaCl buffer at pH 7.0 and at room temperature.

Fig. S8. Fluorescence decrease of EB induced by the competitive binding of complex **1** to CT-DNA in 5 mM Tris-HCl/NaCl buffer (pH 7.0) at room temperature (λ_{ex} = 510 nm, λ_{em} = 588 nm).

Fig. S9. Fluorescence decrease of EB induced by the competitive binding of complex **2** to CT-DNA in 5 mM Tris-HCl/NaCl buffer (pH 7.0) at room temperature (λ_{ex} = 510 nm, λ_{em} = 588 nm).

Fig. S10. Fluorescence decrease of EB induced by the competitive binding of complex **3** to CT-DNA in 5 mM Tris-HCl/NaCl buffer (pH 7.0) at room temperature (λ_{ex} = 510 nm, λ_{em} = 588 nm).

Fig. S11. Fluorescence decrease of EB induced by the competitive binding of complex **4** to CT-DNA in 5 mM Tris-HCl/NaCl buffer (pH 7.0) at room temperature (λ_{ex} = 510 nm, λ_{em} = 588 nm).

Fig. S12. Fluorescence decrease of EB induced by the competitive binding of complex **5** to CT-DNA in 5 mM Tris-HCl/NaCl buffer (pH 7.0) at room temperature (λ_{ex} = 510 nm, λ_{em} = 588 nm).

Fig. S13. Time course of pBR322 DNA cleavage promoted by complex **2** (0.25 mM) at 37 °C and pH 7.00. Inset: agarose GE patterns of the time-variable reaction products. Lanes 1-7, reaction time were 0, 1, 2.5, 4, 5, 6 and 7h, respectively.

Fig. S14. Time course of pBR322 DNA cleavage promoted by complex **2** (0.5 mM) at 37 °C and pH 7.00. Inset: agarose GE patterns of the time-variable reaction products. Lanes 1-7, reaction time were 0, 1, 2, 3, 4, 5 and 6 h, respectively.

Fig. S15. Time course of pBR322 DNA cleavage promoted by complex **2** (0.75 mM) at 37 °C and pH 7.00. Inset: agarose GE patterns of the time-variable reaction products. Lanes 1-7, reaction time were 0, 1, 2, 3, 4, 5 and 6 h, respectively.

Fig. S16. Time course of pBR322 DNA cleavage promoted by complex **2** (1.0 mM) at 37 °C and pH 7.00. Inset: agarose GE patterns of the time-variable reaction products. Lanes 1-7, reaction time were 0, 1, 2, 3, 4, 5 and 6 h, respectively.

Fig. S17. Time course of pBR322 DNA cleavage promoted by complex **2** (1.25 mM) at 37 °C and pH 7.00. Inset: agarose GE patterns of the time-variable reaction products. Lanes 1-7, reaction time were 0, 0.5, 1, 2, 3, 4 and 5 h, respectively.

Fig. S18. Time course of pBR322 DNA cleavage promoted by complex **2** (1.5 mM) at 37 °C and pH 7.00. Inset: agarose GE patterns of the time-variable reaction products. Lanes 1-7, reaction time were 0, 1, 1.5, 2, 2.5, 3 and 4 h, respectively.

Fig. S19. Time course of pBR322 DNA cleavage promoted by complex **2** (1.75 mM) at 37 °C and pH 7.00. Inset: agarose GE patterns of the time-variable reaction products. Lanes 1-7, reaction time were 0, 1, 1.5, 2, 2.5, 3 and 4 h, respectively.

Fig. S20. Time course of pBR322 DNA cleavage promoted by complex **3** (12.5 μM) at 37°C and pH 7.00. Inset: agarose GE patterns of the time-variable reaction products. Lanes 1-7, reaction time were 0, 1, 2.5, 4, 5.5, 7 and 8 h, respectively.

Fig. S21. Time course of pBR322 DNA cleavage promoted by complex **3** (25 μM) at 37°C and pH 7.00. Inset: agarose GE patterns of the time-variable reaction products. Lanes 1-7, reaction time were 0, 1, 2.5, 4, 5, 6 and 7 h, respectively.

Fig. S22. Time course of pBR322 DNA cleavage promoted by complex **3** (37.5 μM) at 37°C and pH 7.00. Inset: agarose GE patterns of the time-variable reaction products. Lanes 1-7, reaction time were 0, 1, 2.5, 4, 5, 6 and 7 h, respectively.

Fig. S23. Time course of pBR322 DNA cleavage promoted by complex **3** (50 μM) at 37°C and pH 7.00. Inset: agarose GE patterns of the time-variable reaction products. Lanes 1-7, reaction time were 0, 1, 2, 3, 4, 5 and 6 h, respectively.

Fig. S24. Time course of pBR322 DNA cleavage promoted by complex **3** (62.5 μM) at 37°C and pH 7.00. Inset: agarose GE patterns of the time-variable reaction products. Lanes 1-7, reaction time were 0, 0.5, 1, 2, 3, 4 and 5 h, respectively.

Fig. S25. Time course of pBR322 DNA cleavage promoted by complex **3** (75 μM) at 37°C and pH 7.00. Inset: agarose GE patterns of the time-variable reaction products. Lanes 1-7, reaction time were 0, 0.5, 1, 2, 3, 4 and 5 h, respectively.

Fig. S26. Time course of pBR322 DNA cleavage promoted by complex **3** (87.5 μM) at 37°C and pH 7.00. Inset: agarose GE patterns of the time-variable reaction products. Lanes 1-7, reaction time were 0, 0.5, 1, 2, 2.5, 3 and 4 h, respectively.

Fig. S27. Time course of pBR322 DNA cleavage promoted by complex **5** (12.5 μM) at 37°C and pH 7.00. Inset: agarose GE patterns of the time-variable reaction products. Lanes 1-7, reaction time were 0, 1, 2.5, 4, 5.5, 7 and 8 h, respectively.

Fig. S28. Time course of pBR322 DNA cleavage promoted by complex **5** (25 μM) at 37°C and pH 7.00. Inset: agarose GE patterns of the time-variable reaction products. Lanes 1-7, reaction time were 0, 1, 2.5, 4, 5, 6 and 7 h, respectively.

Fig. S29. Time course of pBR322 DNA cleavage promoted by complex **5** (37.5 μM) at 37°C and pH 7.00. Inset: agarose GE patterns of the time-variable reaction products. Lanes 1-7, reaction time were 0, 1, 2.5, 4, 5, 6 and 7 h, respectively.

Fig. S30. Time course of pBR322 DNA cleavage promoted by complex **5** (50 μM) at 37°C and pH 7.00. Inset: agarose GE patterns of the time-variable reaction products. Lanes 1-7, reaction time were 0, 1, 2, 3, 4, 5 and 6 h, respectively.

Fig. S31. Time course of pBR322 DNA cleavage promoted by complex **5** (62.5 μM) at 37°C and pH 7.00. Inset: agarose GE patterns of the time-variable reaction products. Lanes 1-7, reaction time were 0, 0.5, 1, 2, 3, 4 and 5 h, respectively.

Fig. S32. Time course of pBR322 DNA cleavage promoted by complex **5** (75 μM) at 37°C and pH 7.00. Inset: agarose GE patterns of the time-variable reaction products. Lanes 1-7, reaction time were 0, 0.5, 1, 2, 3, 4 and 5 h, respectively.

Fig. S33.Time course of pBR322 DNA cleavage promoted by complex **5** (87.5 μM) at 37°C and pH 7.00. Inset: agarose GE patterns of the time-variable reaction products. Lanes 1-7, reaction time were 0, 0.5, 1, 2, 2.5, 3 and 4 h, respectively.

Fig. S34. Agarose GE patterns for the cleavage of pBR322 DNA by complex **2**(1.75 mM) at pH 7.0 and 37 °C for 5 h, in the presence of DMSO (1 M, Lane 3), MeOH (1 M, Lane 4), KI (0.1 M, Lane 5), NaN_3 (0.1 M, Lane 6) and EDTA (0.1 M, Lane 7). Lane 1, DNA alone and Lane 2: DNA + complex **2**.

Fig. S35. Agarose GE patterns for the cleavage of pBR322 DNA by complex **3**(62.5 μM) at pH 7.0 and 37 °C for 5 h, in the presence of DMSO (1 M, Lane 3), MeOH (1 M, Lane 4), KI (0.1 M, Lane 5), NaN_3 (0.1 M, Lane 6) and EDTA (0.1 M, Lane 7). Lane 1, DNA alone and Lane 2: DNA + complex **3**.

Table S1. Selected bond distances (Å) and angles (°) for complexes **1**-**5**.

Complex	Bond	Distance（Å）	Bond	Angles (°)
1	Cu(1)-O(13)	1.8615(18)	O(13)-Cu(1)-O(5)#1	197.54(7)
	Cu(1)-O(2)	1.9237(17)	O(13)-Cu(1)-O(5)#1	97.54(7)
	Cu(2)-O(14)	1.8667(18)	O(5)#1-Cu(1)-O(2)	166.60(7)
	Cu(2)-O(7)	1.9653(18)	O(5)#1-Cu(1)-O(1W)	82.72(8)
	Cu(3)-O(14)	1.8484(18)	O(14)-Cu(2)-O(13)	173.16(10)

	Cu(3)-O(8)	1.9366(16)	O(13)-Cu(2)-O(7)	83.45(8)
	O(5)-Cu(1)#2	1.9101(17)	O(13)-Cu(2)-O(1)	94.46(7)
	Cu(1)-O(5)#1	1.9101(17)	O(14)-Cu(3)-O(11)#2	95.81(8)
	Cu(1)-O(1W)	1.949(2)	O(11)#2-Cu(3)-O(8)	169.14(8)
	Cu(2)-O(13)	1.8786(18)	O(11)#2-Cu(3)-O(2W)	86.42(8)
	Cu(2)-O(1)	1.9874(15)	O(13)-Cu(1)-O(2)	95.82(8)
	Cu(3)-O(11)#2	1.9291(17)	O(13)-Cu(1)-O(1W)	168.16(13)
	Cu(3)-O(2W)	1.9441(19)	O(2)-Cu(1)-O(1W)	83.98(8)
	O(11)-Cu(3)#1	1.9291(17)	O(14)-Cu(2)-O(7)	95.82(8)
			O(14)-Cu(2)-O(1)	85.90(7)
			O(7)-Cu(2)-O(1)	176.34(8)
			O(14)-Cu(3)-O(8)	94.12(8)
			O(14)-Cu(3)-O(2W)	175.74(9)
			O(8)-Cu(3)-O(2W)	83.40(8)
2	Cu(1)-O(1)	1.937(3)	O(1)-Cu(1)-O(1W)	177.90(15)
	Cu(1)-O(5)#3	1.967(3)	O(1)-Cu(1)-O(5)#3	90.98(14)
	Cu(1)-O(2)#4	2.425(3)	O(1W)-Cu(1)-O(5)#3	91.05(14)
	O(2)-Cu(1)#5	2.425(3)	O(1)-Cu(1)-O(2W)	87.32(14)
	Cu(1)-O(1W)	1.944(4)	O(1W)-Cu(1)-O(2W)	90.63(14)
	Cu(1)-O(2W)	1.970(3)	O(5)#3-Cu(1)-O(2W)	176.93(14)
	Cu(1)-H(1W1)	1.86(6)	O(1)-Cu(1)-O(2)#4	85.48(13)
	O(5)-Cu(1)#6	1.967(3)	O(1W)-Cu(1)-O(2)#4	95.10(15)
			O(5)#3-Cu(1)-O(2)#4	88.56(12)
			O(2W)-Cu(1)-O(2)#4	93.86(13)
3	Cu(1)-O(4)#7	1.9452(13)	O(4)#7-Cu(1)-O(2)	95.77(5)
	Cu(1)-N(2)	2.0042(14)	O(2)-Cu(1)-N(2)	172.05(6)
	Cu(1)-O(6)#8	2.4353(15)	O(2)-Cu(1)-N(1)	93.30(6)
	O(6)-Cu(1)#10	2.4353(15)	O(4)#7-Cu(1)-O(6)#8	85.88(6)
	Cu(1)-O(2)	1.9451(12)	N(2)-Cu(1)-O(6)#8	100.88(5)
	Cu(1)-N(1)	2.0112(15)	O(4)#7-Cu(1)-N(2)	89.72(6)
	O(4)-Cu(1)#9	1.9452(13)	O(4)#7-Cu(1)-N(1)	169.29(6)
			N(2)-Cu(1)-N(1)	80.70(6)
			O(2)-Cu(1)-O(6)#8	85.28(5)
			N(1)-Cu(1)-O(6)#8	100.56(5)

Table S1. Continued

Complex	Bond	Distance（Å）	Bond	Angles (°)
4	Cu(1)-O(1)	1.9315(19)	O(1)-Cu(1)-O(1W)	177.15(8)
	Cu(1)-O(6)#11	1.9851(19)	O(1W)-Cu(1)-O(6)#11	92.15(9)
	Cu(1)-O(5)#12	2.293(2)	O(1W)-Cu(1)-O(2W)	92.08(8)
	O(6)-Cu(1)#13	1.9851(19)	O(5)#11-Cu(1)-O(1W)	82.72(8)
	Cu(1)-O(1W)	1.936(2)	O(1)-Cu(1)-O(5)#12	92.39(8)

	Cu(1)-O(2W)	1.9893(19)	O(1)-Cu(1)-O(5)#12	11.98(8)
	O(5)-Cu(1)#12	2.293(2)	O(1)-Cu(1)-O(6)#11	90.62(8)
			O(1)-Cu(1)-O(2W)	85.14(8)
			O(6)#11-Cu(1)-O(2W)	151.62(9)
			O(1W)-Cu(1)-O(5)#12	87.21(9)
			O(2W)-Cu(1)-O(5)#12	96.24(8)
5	Cu(1)-O(5)#14	1.944(4)	O(5)#14-Cu(1)-O(1)	94.31(17)
	Cu(1)-N(1)	2.020(5)	O(1)-Cu(1)-N(1)	164.42(19)
	Cu(1)-O(1W)	2.271(4)	O(1)-Cu(1)-N(2)	96.72(18)
	Cu(1)-O(1)	1.975(4)	O(5)#14-Cu(1)-O(1W)	84.42(18)
	Cu(1)-N(2)	2.027(5)	N(1)-Cu(1)-O(1W)	108.30(19)
	O(5)-Cu(1)#15	1.944(4)	O(5)#14-Cu(1)-N(1)	96.24(8)
			O(5)#14-Cu(1)-N(2)	165.32(18)
			N(1)-Cu(1)-N(2)	81.6(2)
			O(1)-Cu(1)-O(1W)	86.98(17)
			N(2)-Cu(1)-O(1W)	86.51(18)

Symmetry transformations used to generate equivalent atoms: #1: *x* + 1, *y* + 1, *z*; #2: *x* - 1, *y* - 1, *z*; #3: *x* + 1, *y*, *z*; #4: -*x* + 1, *y* + 1/2, -*z* + 1/2; #5: -*x* + 1, *y* - 1/2, -*z* + 1/2 ; #6: *x* - 1, *y*, *z*; #7: *x* + 1, *y*, *z*; #8: -*x* + 1/2, *y* + 1/2, -*z* + 3/2; #9: *x* - 1, *y*, *z*; #10: -*x* + 1/2, *y* - 1/2, -*z* + 3/2; #11: *x* + 1, *y* -1 , *z*; #12: -*x* - 2, -*y* + 2, -z + 1; #13: x-1,y+1,z; #14: *x* - 1, *y*, z; #15: *x* + 1, *y*, *z*.

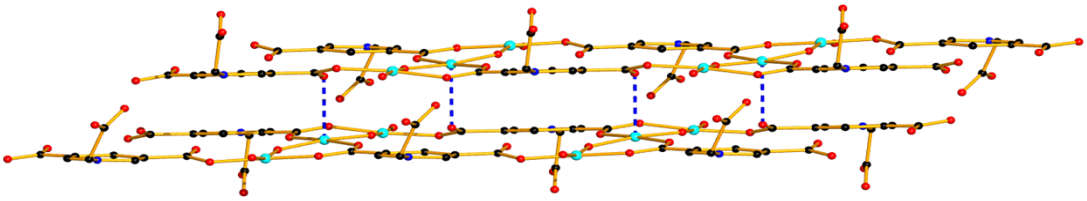

Fig. S1. The double layered structure linked by secondary bond of Cu···O in $\{[Cu_3(Cmdcp)_2(HO)_2(H_2O)_2]\cdot H_2O\}_n$ (**1**).

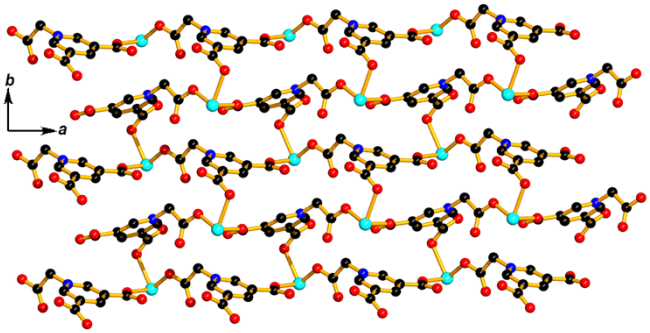

Fig. S2. The infinite two-dimensional structure in **3** looking along the *c* axis and all the hydrogen atoms and bipy molecules are omitted for clarity.

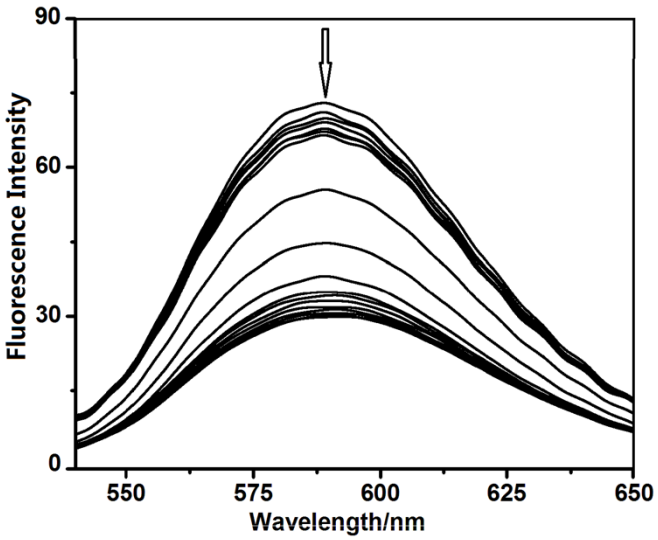

Fig. S3. The effect of the addition of complex **1** on the emission intensity of the CT DNA-bound ethidium bromide (3.03 μM) at different complex concentrations in a 5 mM Tri-HCl-50 mM NaCl buffer at pH 7.0 and at room temperature.

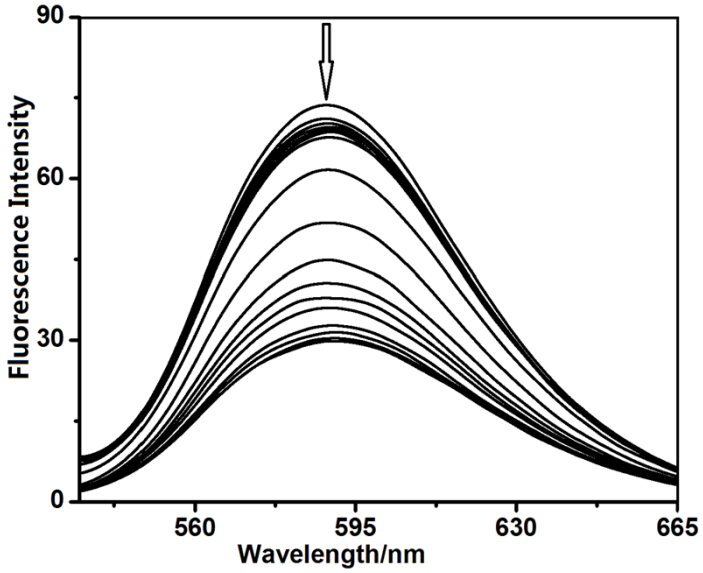

Fig. S4. The effect of the addition of complex **2** on the emission intensity of the CT DNA-bound ethidium bromide (3.03 μM) at different complex concentrations in a 5 mM Tri-HCl-50 mM NaCl buffer at pH 7.0 and at room temperature.

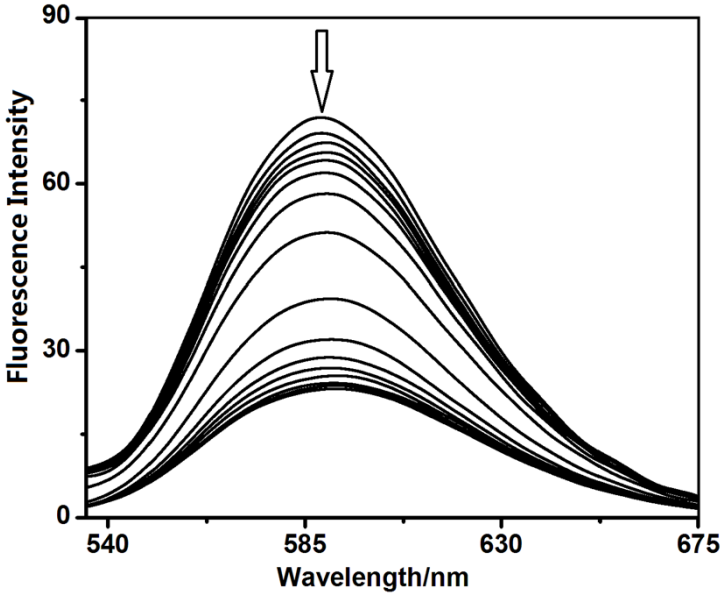

Fig. S5. The effect of the addition of complex **3** on the emission intensity of the CT DNA-bound ethidium bromide (3.03 μM) at different complex concentrations in a 5 mM Tri-HCl-50 mM NaCl buffer at pH 7.0 and at room temperature.

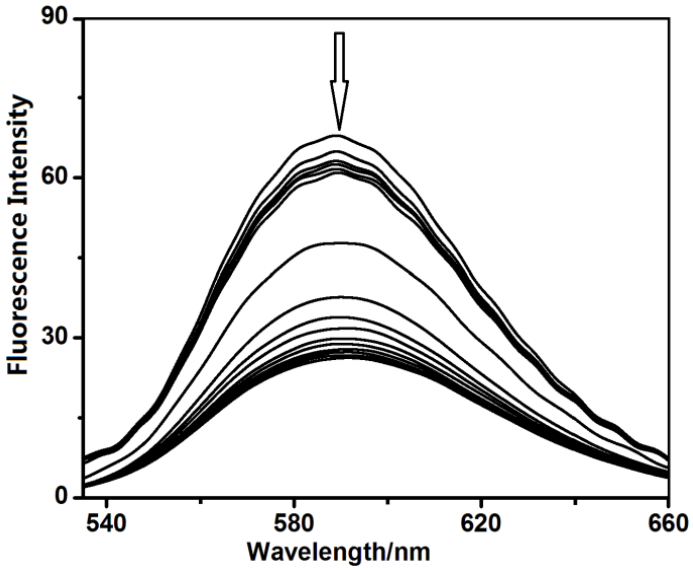

Fig. S6. The effect of the addition of complex **4** on the emission intensity of the CT DNA-bound ethidium bromide (3.03 μM) at different complex concentrations in a 5 mM Tri-HCl-50 mM NaCl buffer at pH 7.0 and at room temperature.

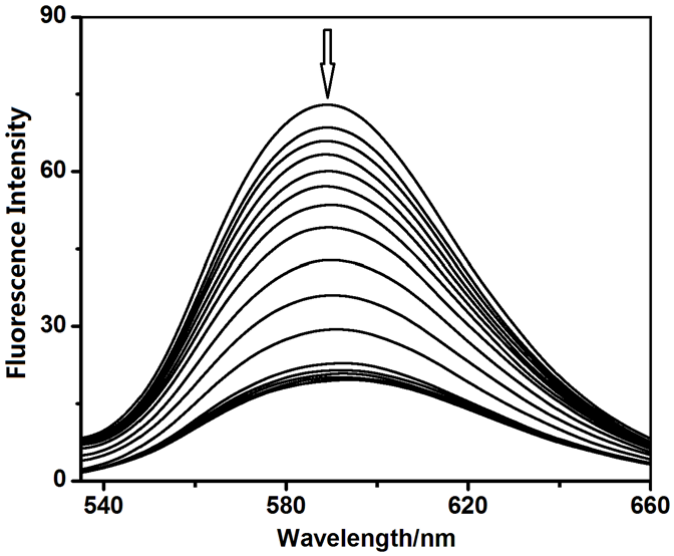

Fig. S7. The effect of the addition of complex **5** on the emission intensity of the CT DNA-bound ethidium bromide (3.03 μM) at different complex concentrations in a 5 mM Tri-HCl-50 mM NaCl buffer at pH 7.0 and at room temperature.

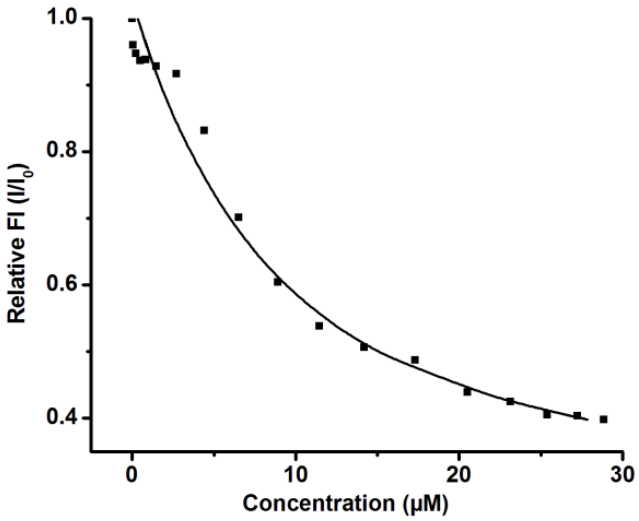

Fig. S8. Fluorescence decrease of EB induced by the competitive binding of complex **1** to CT-DNA in 5 mM Tris-HCl/NaCl buffer (pH 7.0) at room temperature (λ_{ex} = 510 nm, λ_{em} = 588 nm).

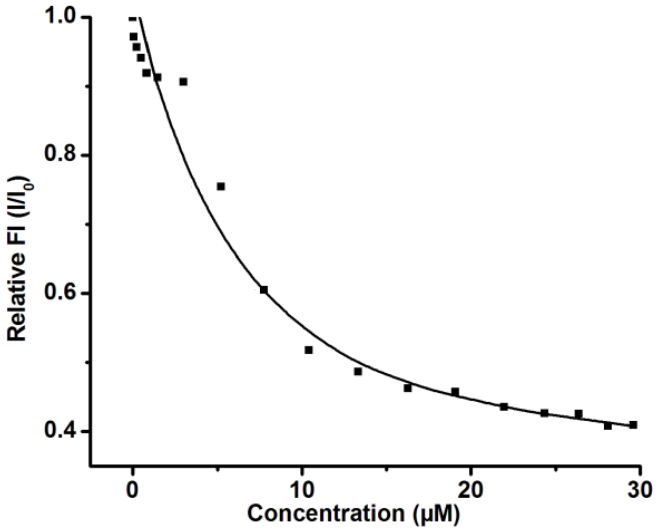

Fig. S9. Fluorescence decrease of EB induced by the competitive binding of complex **2** to CT-DNA in 5 mM Tris-HCl/NaCl buffer (pH 7.0) at room temperature (λ_{ex} = 510 nm, λ_{em} = 588 nm).

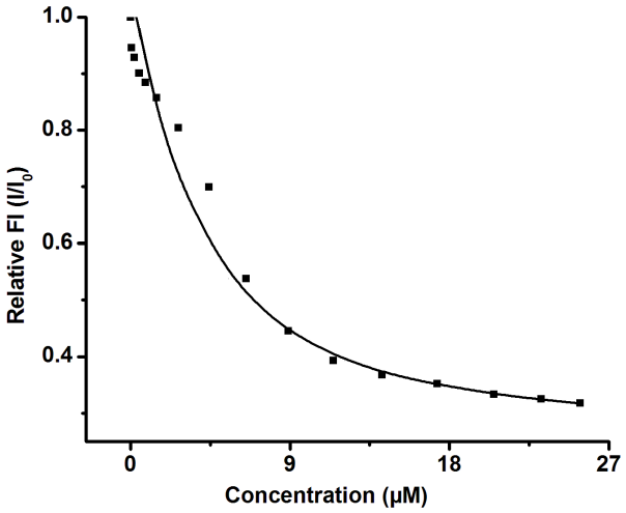

Fig. S10. Fluorescence decrease of EB induced by the competitive binding of complex **3** to CT-DNA in 5 mM Tris-HCl/NaCl buffer (pH 7.0) at room temperature (λ_{ex} = 510 nm, λ_{em} = 588 nm).

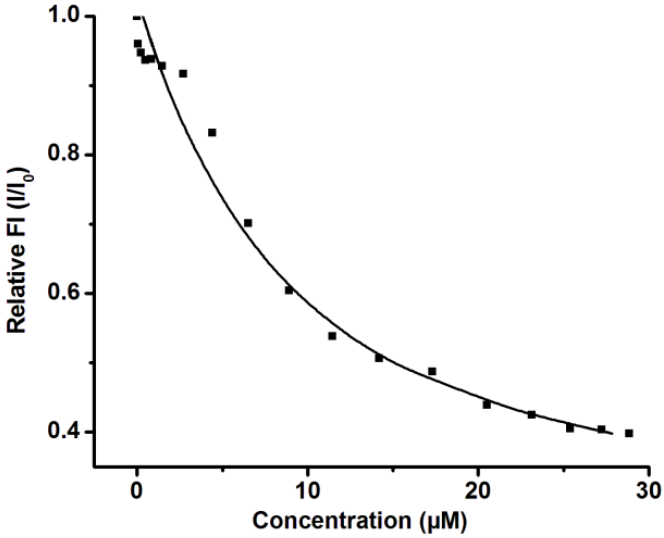

Fig. S11. Fluorescence decrease of EB induced by the competitive binding of complex **4** to CT-DNA in 5 mM Tris-HCl/NaCl buffer (pH 7.0) at room temperature (λ_{ex} = 510 nm, λ_{em} = 588 nm).

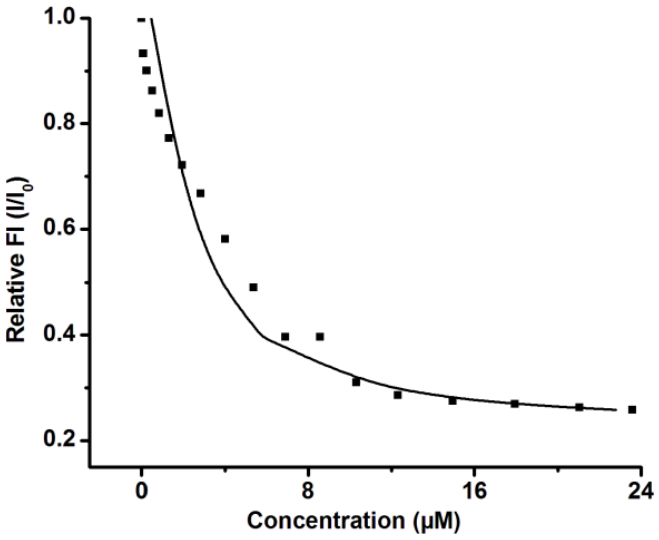

Fig. S12. Fluorescence decrease of EB induced by the competitive binding of complex **5** to CT-DNA in 5 mM Tris-HCl/NaCl buffer (pH 7.0) at room temperature (λ_{ex} = 510 nm, λ_{em} = 588 nm).

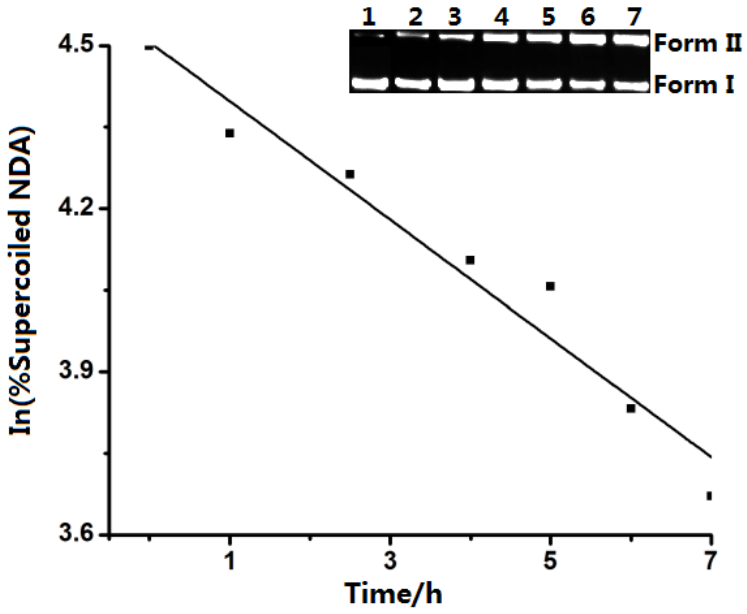

Fig. S13. Time course of pBR322 DNA cleavage promoted by complex **2** (0.25 mM) at 37°C and pH 7.00. Inset: agarose GE patterns of the time-variable reaction products. Lanes 1-7, reaction time were 0, 1, 2.5, 4, 5, 6 and 7 h, respectively.

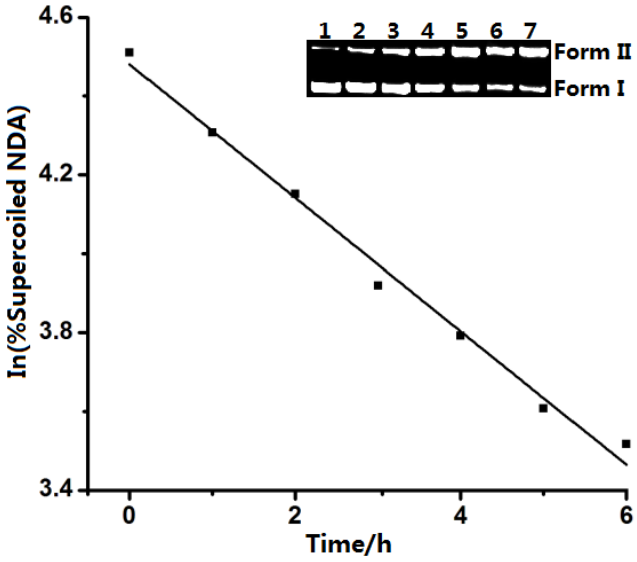

Fig. S14. Time course of pBR322 DNA cleavage promoted by complex **2** (0.5 mM) at 37°C and pH 7.00. Inset: agarose GE patterns of the time-variable reaction products. Lanes 1-7, reaction time were 0, 1, 2, 3, 4, 5 and 6 h, respectively.

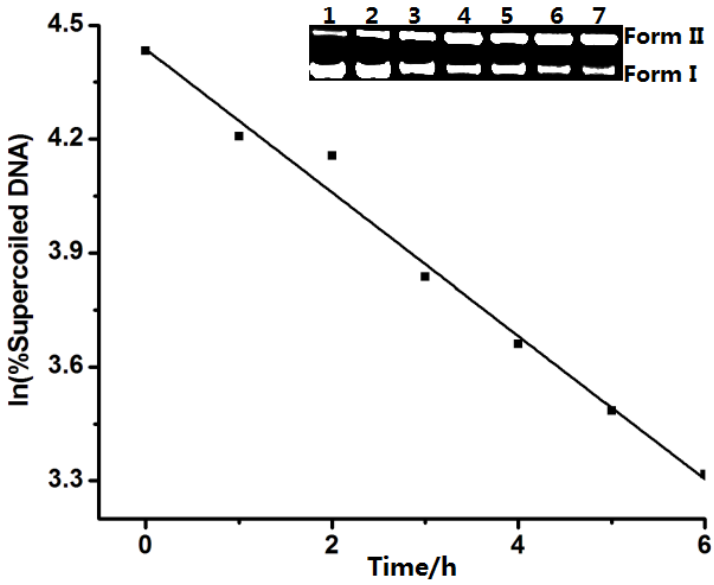

Fig. S15. Time course of pBR322 DNA cleavage promoted by complex **2** (0.75 mM) at 37°C and pH 7.00. Inset: agarose GE patterns of the time-variable reaction products. Lanes 1-7, reaction time were 0, 1, 2, 3, 4, 5 and 6 h, respectively.

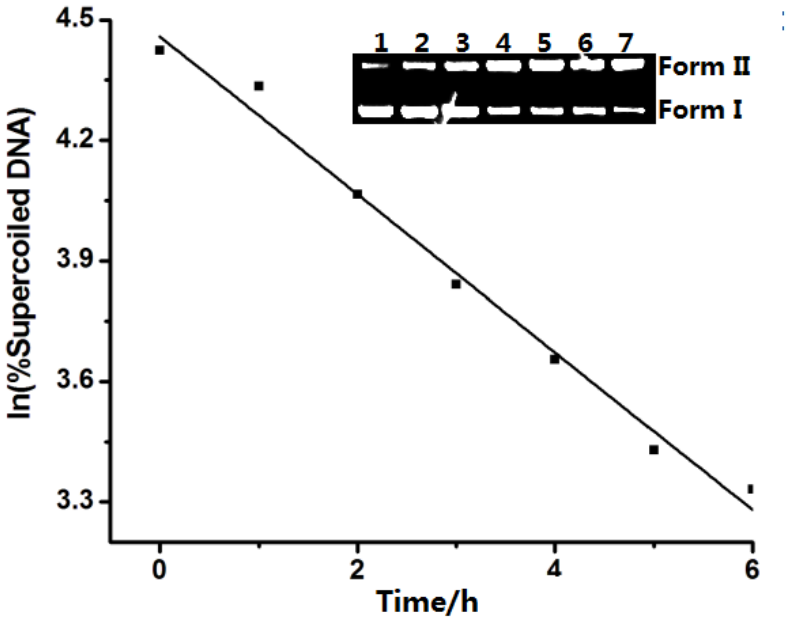

Fig. S16. Time course of pBR322 DNA cleavage promoted by complex **2** (1.0 mM) at 37°C and pH 7.00. Inset: agarose GE patterns of the time-variable reaction products. Lanes 1-7, reaction time were 0, 1, 2, 3, 4, 5 and 6 h, respectively.

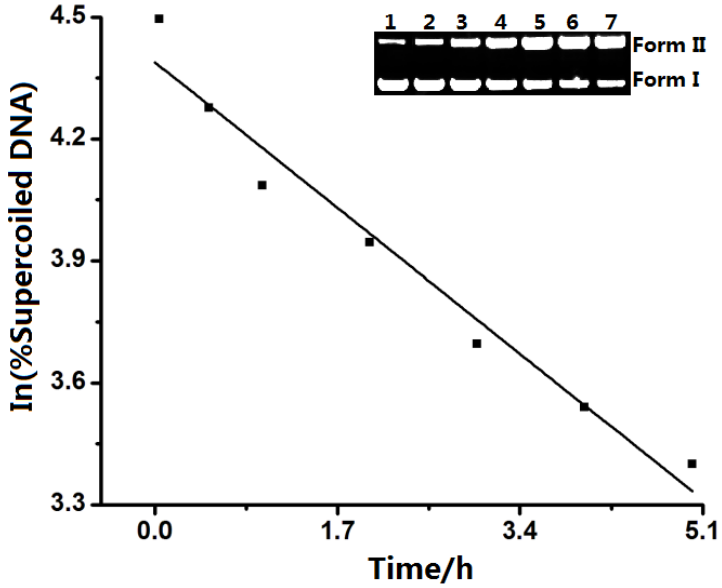

Fig. S17. Time course of pBR322 DNA cleavage promoted by complex **2** (1.25 mM) at 37°C and pH 7.00. Inset: agarose GE patterns of the time-variable reaction products. Lanes 1-7, reaction time were 0, 0.5, 1, 2, 3, 4 and 5 h, respectively.

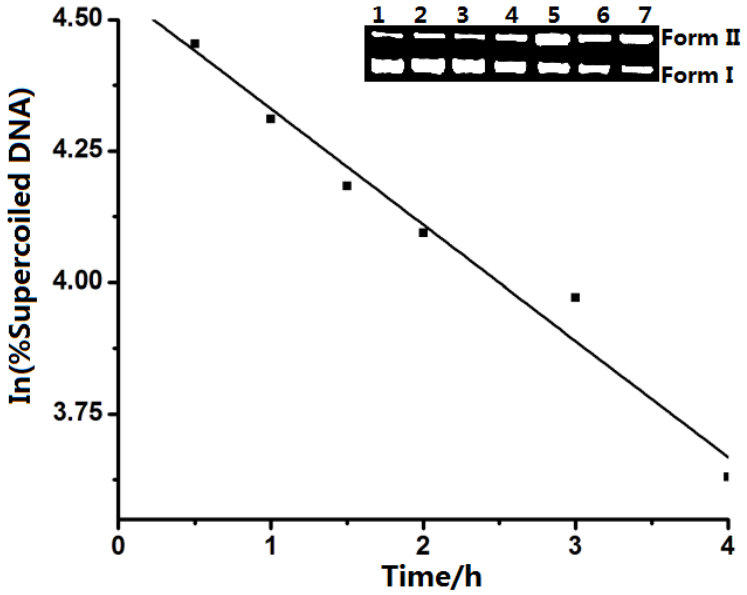

Fig. S18. Time course of pBR322 DNA cleavage promoted by complex **2** (1.5 mM) at 37°C and pH 7.00. Inset: agarose GE patterns of the time-variable reaction products. Lanes 1-7, reaction time were 0, 0.5, 1, 1.5, 2, 3 and 4 h, respectively.

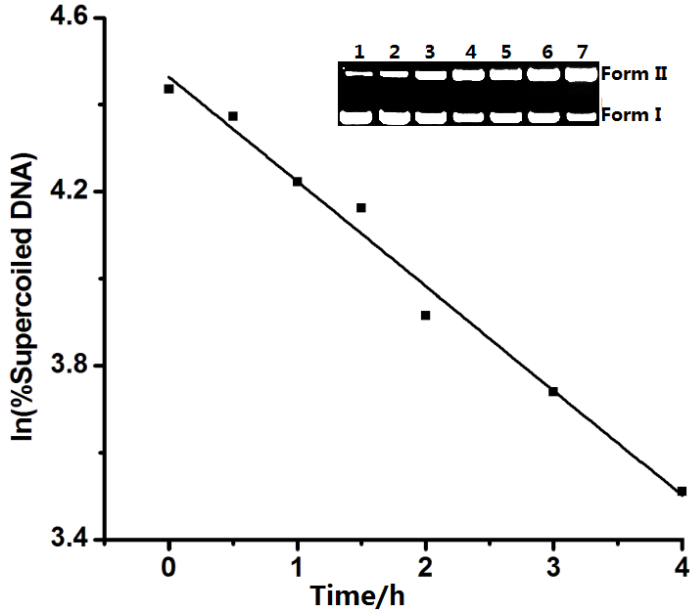

Fig. S19. Time course of pBR322 DNA cleavage promoted by complex **2** (1.75 mM) at 37°C and pH 7.00. Inset: agarose GE patterns of the time-variable reaction products. Lanes 1-7, reaction time were 0, 0.5, 1, 1.5, 2, 3 and 4 h, respectively.

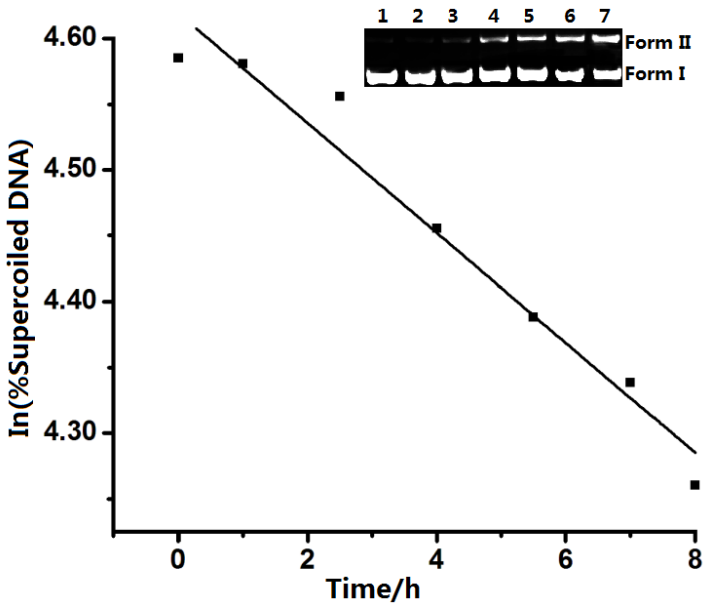

Fig. S20. Time course of pBR322 DNA cleavage promoted by complex **3** (12.5 μM) at 37°C and pH 7.00. Inset: agarose GE patterns of the time-variable reaction products. Lanes 1-7, reaction time were 0, 1, 2.5, 4, 5.5, 7 and 8 h, respectively.

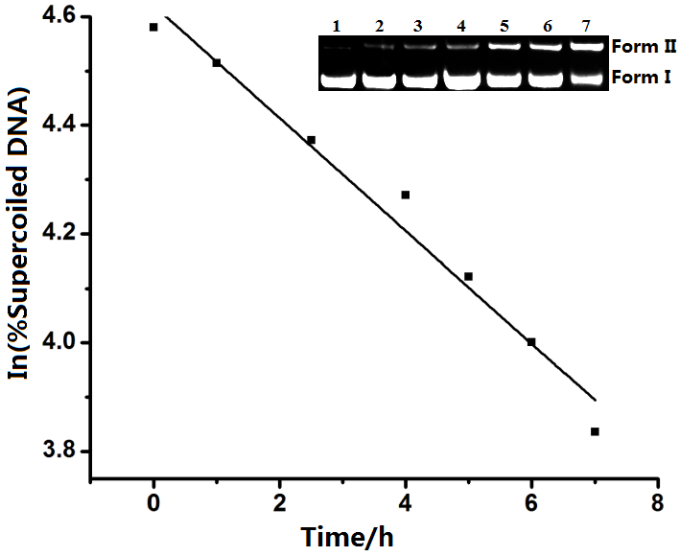

Fig. S21. Time course of pBR322 DNA cleavage promoted by complex **3** (25 μM) at 37°C and pH 7.00. Inset: agarose GE patterns of the time-variable reaction products. Lanes 1-7, reaction time were 0, 1, 2.5, 4, 5, 6 and 7 h, respectively.

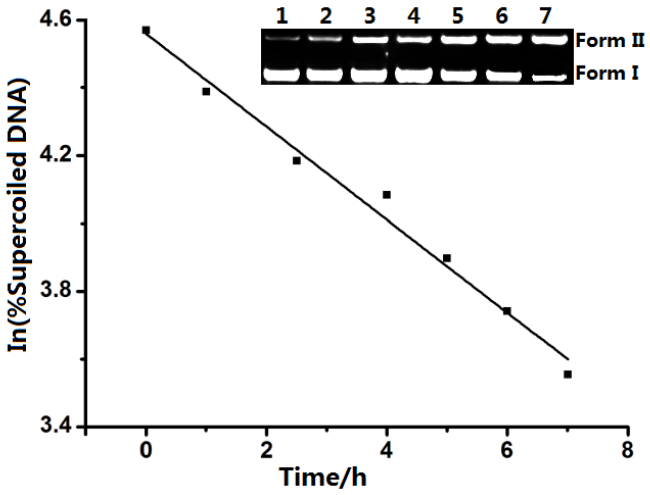

Fig. S22. Time course of pBR322 DNA cleavage promoted by complex **3** (37.5 μM) at 37°C and pH 7.00. Inset: agarose GE patterns of the time-variable reaction products. Lanes 1-7, reaction time were 0, 1, 2.5, 4, 5, 6 and 7 h, respectively.

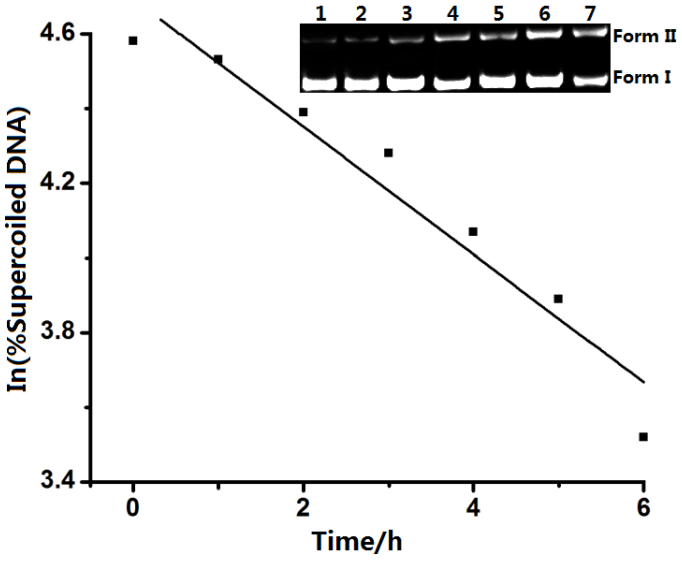

Fig. S23. Time course of pBR322 DNA cleavage promoted by complex **3** (50 μM) at 37°C and pH 7.00. Inset: agarose GE patterns of the time-variable reaction products. Lanes 1-7, reaction time were 0, 1, 2, 3, 4, 5 and 6 h, respectively.

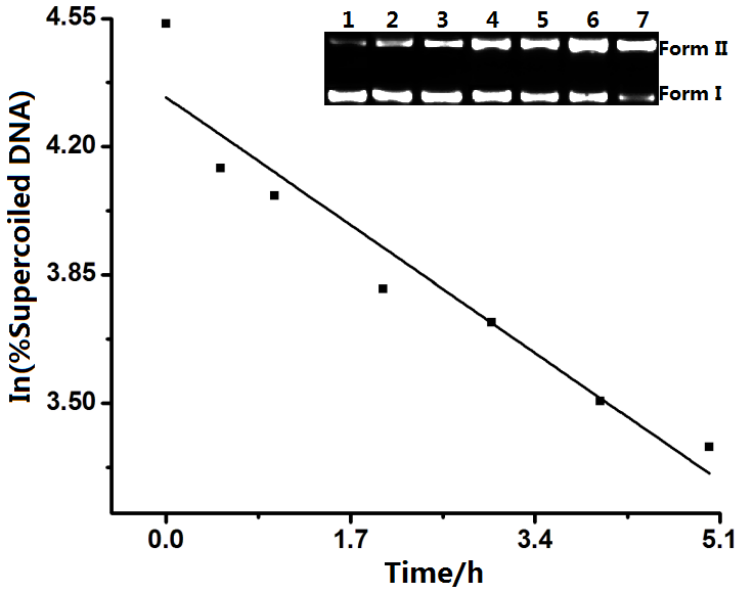

Fig. S24. Time course of pBR322 DNA cleavage promoted by complex **3** (62.5 μM) at 37°C and pH 7.00. Inset: agarose GE patterns of the time-variable reaction products. Lanes 1-7, reaction time were 0, 0.5, 1, 2, 3, 4 and 5 h, respectively.

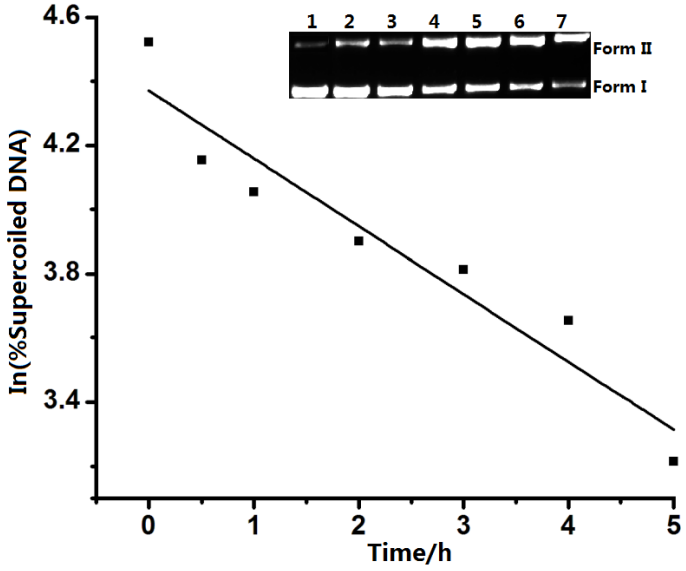

Fig. S25. Time course of pBR322 DNA cleavage promoted by complex **3** (75 μM) at 37°C and pH 7.00. Inset: agarose GE patterns of the time-variable reaction products. Lanes 1-7, reaction time were 0, 0.5, 1, 2, 3, 4 and 5 h, respectively.

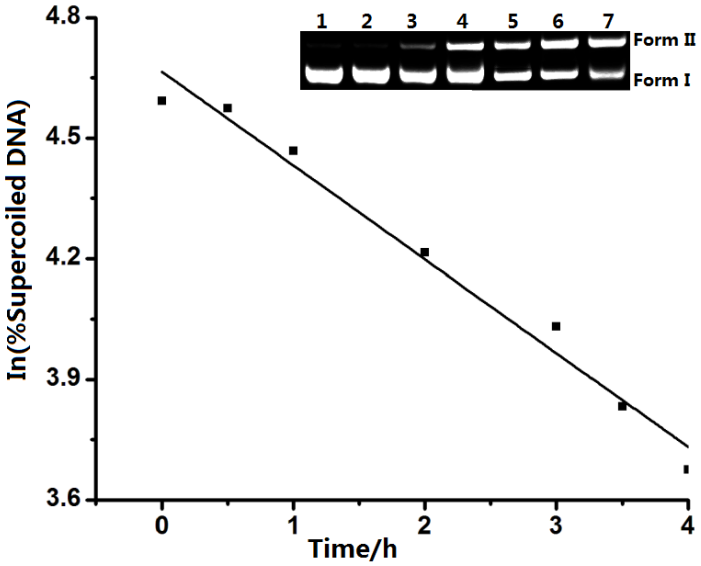

Fig. S26. Time course of pBR322 DNA cleavage promoted by complex **3** (87.5 μM) at 37°C and pH 7.00. Inset: agarose GE patterns of the time-variable reaction products. Lanes 1-7, reaction time were 0, 0.5, 1, 2, 2.5, 3 and 4 h, respectively.

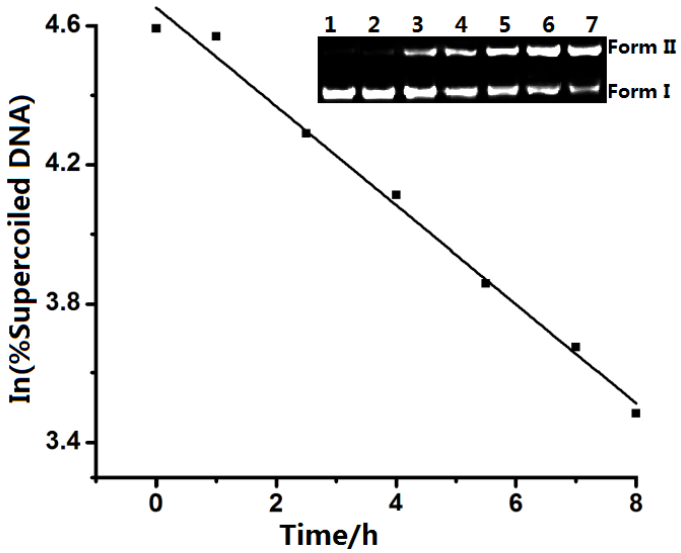

Fig. S27. Time course of pBR322 DNA cleavage promoted by complex **5** (12.5 μM) at 37°C and pH 7.00. Inset: agarose GE patterns of the time-variable reaction products. Lanes 1-7, reaction time were 0, 1, 2.5, 4, 5.5, 7 and 8 h, respectively.

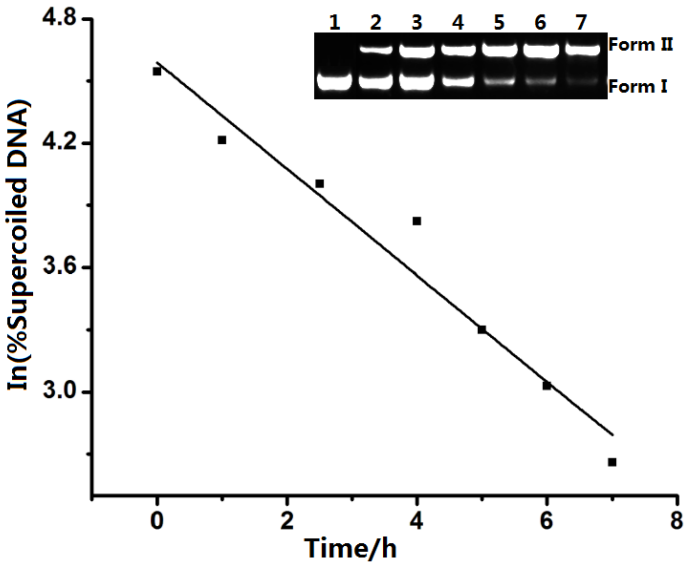

Fig. S28. Time course of pBR322 DNA cleavage promoted by complex **5** (25 μM) at 37°C and pH 7.00. Inset: agarose GE patterns of the time-variable reaction products. Lanes 1-7, reaction time were 0, 1, 2.5, 4, 5, 6 and 7 h, respectively.

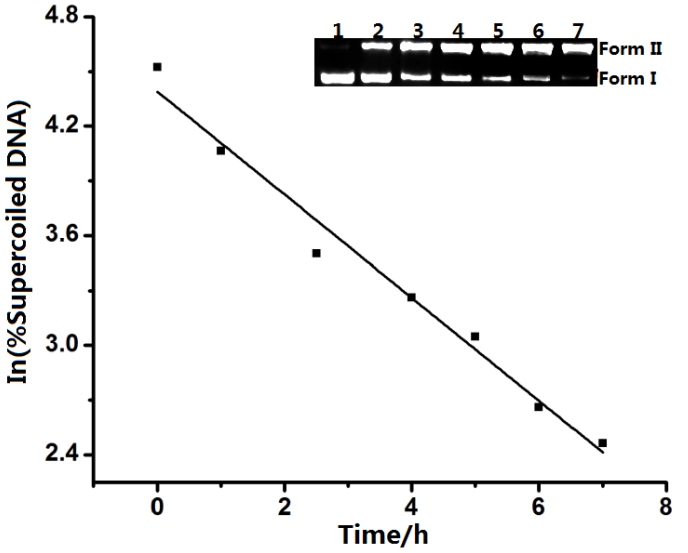

Fig. S29. Time course of pBR322 DNA cleavage promoted by complex **5** (37.5 μM) at 37°C and pH 7.00. Inset: agarose GE patterns of the time-variable reaction products. Lanes 1-7, reaction time were 0, 1, 2.5, 4, 5, 6 and 7 h, respectively.

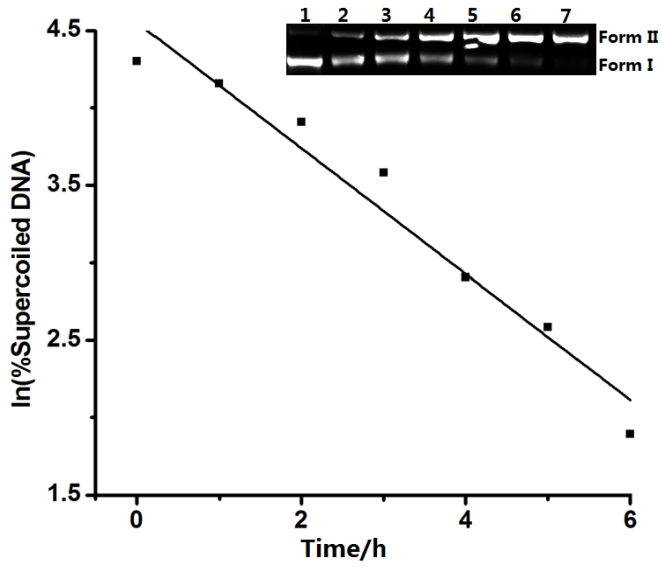

Fig. S30. Time course of pBR322 DNA cleavage promoted by complex **5** (50 μM) at 37°C and pH 7.00. Inset: agarose GE patterns of the time-variable reaction products. Lanes 1-7, reaction time were 0, 1, 2, 3, 4, 5 and 6 h, respectively.

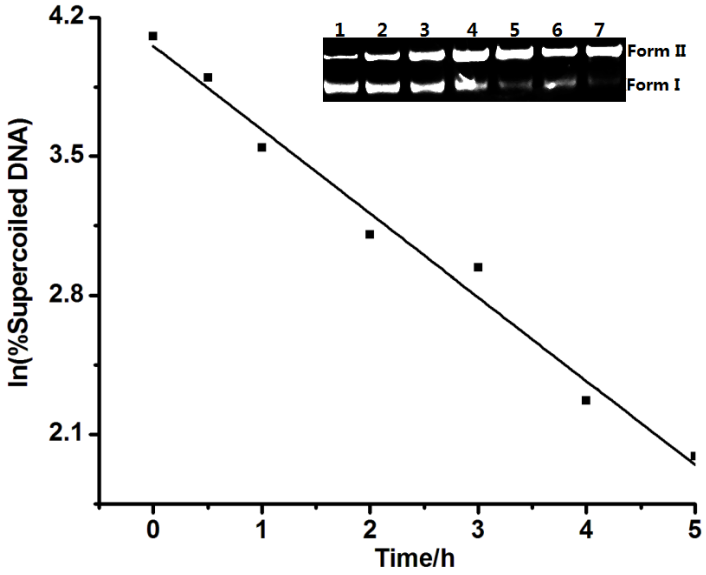

Fig. S31. Time course of pBR322 DNA cleavage promoted by complex **5** (62.5 μM) at 37°C and pH 7.00. Inset: agarose GE patterns of the time-variable reaction products. Lanes 1-7, reaction time were 0, 0.5, 1, 2, 3, 4 and 5 h, respectively.

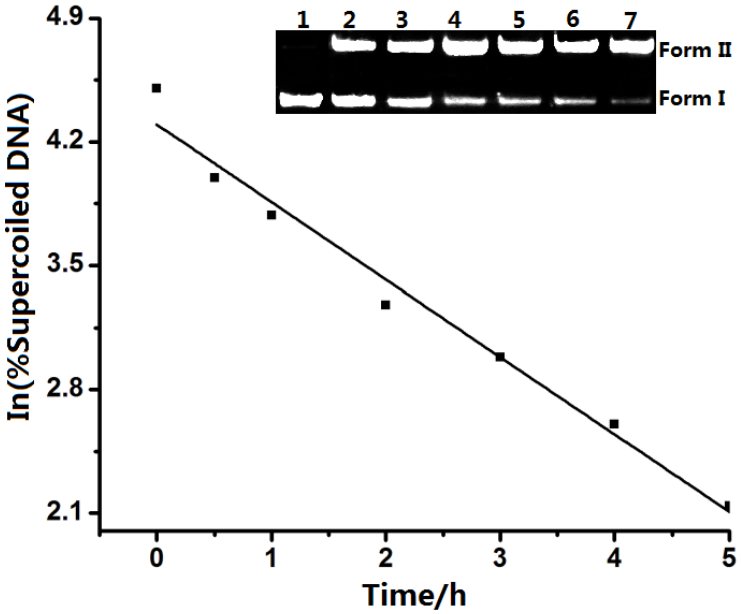

Fig. S32. Time course of pBR322 DNA cleavage promoted by complex **5** (75 μM) at 37°C and pH 7.00. Inset: agarose GE patterns of the time-variable reaction products. Lanes 1-7, reaction time were 0, 0.5, 1, 2, 3, 4 and 5 h, respectively.

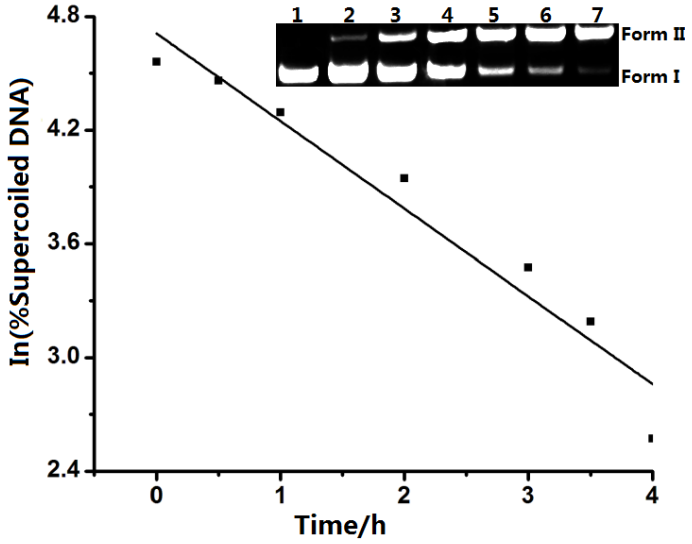

Fig. S33. Time course of pBR322 DNA cleavage promoted by complex **5** (87.5 μM) at 37°C and pH 7.00. Inset: agarose GE patterns of the time-variable reaction products. Lanes 1-7, reaction time were 0, 0.5, 1, 2, 2.5, 3 and 4 h, respectively.

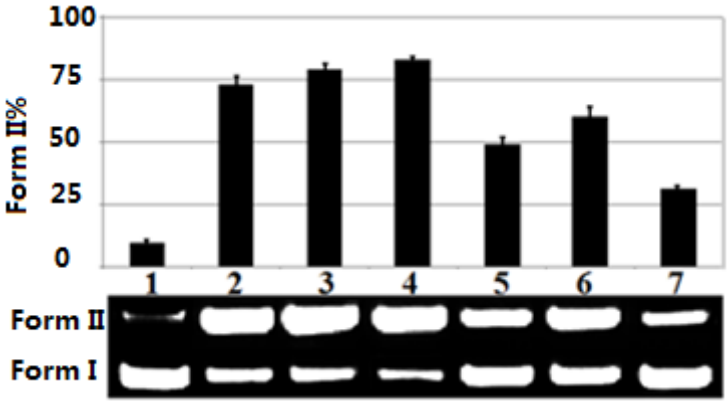

Fig. S34. Agarose GE patterns for the cleavage of pBR322 DNA by complex **2** (1.75 mM) at pH 7.0 and 37°C for 5 h, in the presence of DMSO (1 M, Lane 3), MeOH (1 M, Lane4), KI (0.1 M, Lane 5), NaN_3 (0.1 M, Lane 6) and EDTA (0.1 M, Lane 7). Lane 1, DNA alone and Lane 2: DNA + complex **2**.

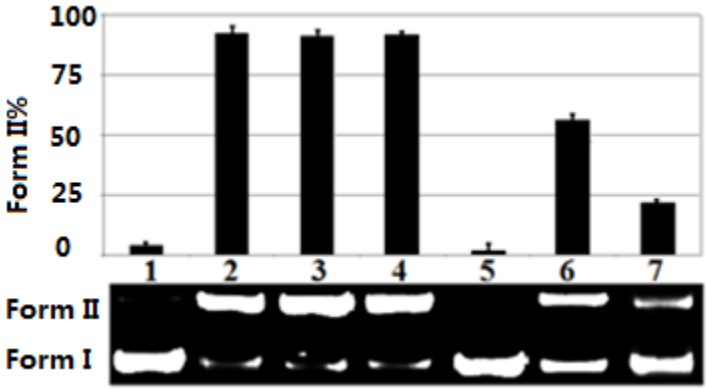

Fig. S35. Agarose GE patterns for the cleavage of pBR322 DNA by complex **3** (62.5 μM) at pH 7.0 and 37°C for 5 h, in the presence of DMSO (1 M, Lane 3), MeOH (1 M, Lane4), KI (0.1 M, Lane 5), NaN_3 (0.1 M, Lane 6) and EDTA (0.1 M, Lane 7). Lane 1, DNA alone and Lane 2: DNA + complex **3**.